doi:10.1016/j.jmb.2004.09.073 J. Mol. Biol. (2004) 344, 965–976

JMB

Available online at www.sciencedirect.com

SCIENCE DIRECT®

ELSEVIER

Efficient Attenuation of Stochasticity in Gene Expression Through Post-transcriptional Control

Peter S. Swain

Centre for Non-linear Dynamics, Department of Physiology, McGill University 3655 Promenade Sir William Osler, Montreal, Que., Canada H3G 1Y6

Thermal fluctuations can lead to significant, unpredictable concentration changes in intracellular molecules, potentially disrupting the functioning of cellular networks and challenging cellular efficiency. Biochemical systems might therefore be expected to have evolved network architectures and motifs that limit the effects of stochastic disturbances. During gene expression itself, stochasticity, or "noise", in protein concentrations is believed to be determined mostly by mRNA, rather than protein, levels. Here, we demonstrate *in silico*, and analytically, how a number of commonly occurring network architectures in bacteria use mRNA to efficiently attenuate fluctuations. Genes coded in operons share mRNA, which we show generates strongly correlated expression despite multiple ribosome binding sites. For autogeneous control, we provide general analytic expressions using Langevin theory, and demonstrate that negative translational feedback has a much greater efficiency at reducing stochasticity than negative transcriptional feedback. Using the ribosomal proteins as an example, we also show that translational, rather than transcriptional, feedback best coordinates gene expression during assembly of macromolecular complexes. Our findings suggest that selection of a gene controlled post-transcriptionally may be for the resulting low stochasticity in its expression. Such low noise genes can be speculated to play a central role in the local gene network.

Keywords: stochastic gene expression; post-transcriptional control; negative feedback; macromolecular complexes; computational modelling

Introduction

In many cells, and especially in bacteria, it is likely that small numbers of molecules are frequently involved in effecting cellular processes.[1] Such small numbers lead to the stochasticity that is inherent in any chemical reaction becoming significant, and the cellular milieu becoming "noisy".[2] Noise implies that protein and RNA numbers can tend far from their mean values, and so cellular information processing must function through biochemical networks whose components potentially fluctuate significantly and unpredictably. To circumvent this problem, one might expect that *in vivo* signal transduction and genetic networks have network architectures that have partly evolved to limit noise, at least in their key molecular "players". For example, it has been argued that the genetic networks underlying circadian rhythms have a structure that hinders biochemical stochasticity from disrupting the period of the circadian clock.[3,4] Dimerization of transcription factors[5] and DNA looping[6] may also act to attenuate noise. For signal transduction systems, protein cascades have been theoretically shown to reduce the propagation of noise arising from a fluctuating cascade input.[7] However, the magnitude of the (intrinsic) noise for a particular protein is expected to be mostly set by levels of mRNA, rather than those of protein itself.[8,9] Here, we demonstrate the importance of that finding for efficient noise reduction in genetic networks *via* some simple, commonly found, network motifs.

Intrinsic Noise

Two molecules must first find each other in the cell and overcome an energy barrier before they can interact. Thermal fluctuations cause this process not

Abbreviations used: RNAP, RNA polymerase; RBS, ribosome-binding site; nt, nucleotide.

E-mail address of the corresponding author: swain@cnd.mcgill.ca

to happen continuously and deterministically, but to occur with a finite probability per unit time. Chemical reactions are, thus, inherently stochastic, and we refer to this stochasticity as intrinsic noise. Fluctuating extrinsic quantities are another source of noise. These variables, although not necessarily exterior to the cell, do develop exterior to the system of interest and yet still act on it. Such a system may be, for example, one gene or an entire gene network. For the two or three gene systems we will consider, extrinsic variables usually affect all genes in the system equally, and include, for example, the numbers of RNA polymerases (RNAPs) and ribosomes, and the extracellular environment. We will not explicitly describe such extrinsic effects.

We define the noise, η, of any distribution to be its standard deviation divided by its mean, i.e. the size of a typical fluctuation compared to the mean value. For a simple model of constitutive expression, which includes only intrinsic effects and is detailed in Figure 1(b), the noise obeys:[8,10]

$$\eta^2_{\text{con}} = \frac{1}{\langle A\rangle_{\text{con}}} + \frac{d_1}{d_0 + d_1}\frac{1}{\langle M\rangle_{\text{con}}} \tag{1}$$

where A and M are protein and mRNA numbers, and d_1 and d_0 are protein and mRNA degradation rates, respectively. The mRNA term, which is the noise in mRNA effectively scaled by the ratio of the mRNA life-time (typically minutes) to the protein life-time (typically hours), usually dominates; mean mRNA numbers are often much less than mean protein numbers. Equation (1) implies that noise is reduced for proteins that live much longer than mRNA, as each protein is then able to average over many mRNA fluctuations.

For two proteins, A_1 and A_2, expressed from genes with the same types of promoter and ribosome-binding site (RBS), the intrinsic noise (for that promoter and RBS system) is defined as:[2]

$$\eta^2_{\text{int}} = \frac{\langle (A_1 - A_2)^2\rangle}{2\langle A_1\rangle\langle A_2\rangle} \tag{2}$$

Equation (2) is a normalized measure of the dissimilarity in protein concentrations. A constitutive system, with independent expression of A_1 and A_2 and no fluctuating extrinsic variables, has no extrinsic noise; it generates identical distributions of A_1 and A_2, and has an intrinsic noise given by (1). Experimentally, the intrinsic noise has been measured to be as high as 0.6 in *Escherichia coli*, implying that fluctuations typically shift proteins to approximately 60% below or above their mean values.[2]

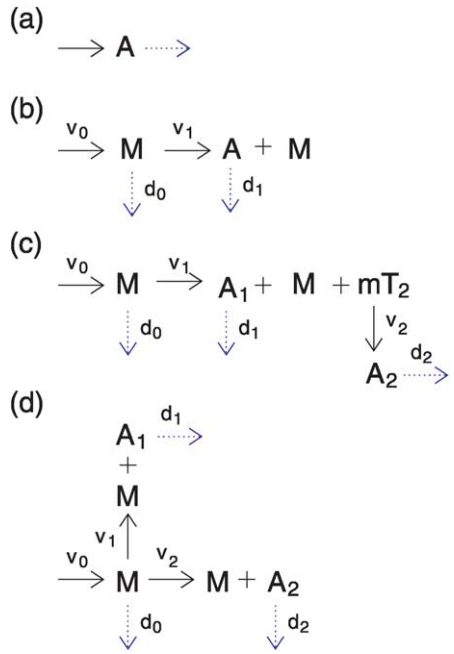

Figure 1. Reaction models for constitutive expression. Protein and mRNA are denoted by A and M, respectively. Transcription is labelled by v_0 and translation by both v_1 and v_2. All degradation reactions are marked by a d_i and a dotted arrow. (a) A "birth-and-death" model. The resulting steady-state protein distribution is Poisson. (b) Constitutive expression. Translation (rate v_1) copies and does not deplete mRNA. (c) Two cistron "read-through" operon with protein products A_1 and A_2. The mRNA has just one RBS. Ribosomes move directly from the first to the second gene, and mT_2 denotes a ribosome translating the second gene. (d) Two cistron operon with two independent RBSs.

Polycistronic mRNAs

Transcription sets mRNA levels, which principally set stochasticity. The intrinsic noise between two proteins will therefore be significantly reduced if their mRNA fluctuations can be correlated. One way to generate such correlation is to encode both proteins on the same mRNA (polycistronic mRNA), an approach frequently adopted by bacteria through the use of operons. Polycistronic mRNA ensures that the mRNA fluctuations associated with each of the two proteins have almost perfect correlations. Such mRNA may have only one RBS; the start of the coding for protein A_2 can be close enough to the end of the coding for protein A_1 that a ribosome can immediately "read-through" to the A_2 coding region after releasing an A_1.[11] A model for such a scheme is shown in Figure 1(c). By solving for the moments of a master equation,[12] the intrinsic noise can be shown to be:

$$\eta^2_{\text{1RBS}} = \frac{1}{\langle A\rangle} - \frac{d_1}{2(d_0 + d_1)}\frac{1}{\langle M\rangle} \times \frac{d_0(d_0 + v_1) + d_1 v_1}{(d_0 + v_1)(d_1 + v_1)} \tag{3}$$

where v_1 is the rate of translation (of order 0.01 s^{-1}), and the rate constants for A_1 and A_2 expression have been chosen to be equal implying that $\langle A_1\rangle = \langle A_2\rangle \equiv \langle A\rangle$. A comparison of (3) with (1) shows immediately that the noise is significantly reduced by the polycistronic structure through the negative

term in (3). In fact, as $d_1 \ll d_0$, a series expansion of (3), for small d_1, shows that $\eta^2_{1\mathrm{RBS}} \simeq 1/(2\langle A\rangle)$.

To gain some understanding of (3), it is instructive to consider the very simple model of gene expression shown in Figure 1(a). Here, protein is synthesized with a constant probability per unit time and degrades in a first-order manner. The resulting distribution in protein number is Poisson, and the noise squared, η^2, is $1/\langle A\rangle$. For two proteins, independently expressed through identically parameterized Poisson processes, the intrinsic noise squared is again just $1/\langle A\rangle$, as there are no fluctuating extrinsic variables. The negative term in (3), thus, reduces the intrinsic noise below the Poisson result. Unlike in a Poisson model, where synthesis of A_1 and A_2 are independent, every time an A_1 protein is synthesized in the scheme of Figure 1(c), an A_2 protein must also be synthesized. This additional correlation reduces the intrinsic noise.

A polycistronic mRNA may have more than one RBS and independent translation of each of the genes it encodes. Such a scheme is shown in Figure 1(d), for which the intrinsic noise is given by:

$$\eta^2_{2\mathrm{RBS}} = \frac{1}{\langle A\rangle} \tag{4}$$

when, for simplicity, the parameters are set to $v_2 = v_1$ and $d_2 = d_1$. The intrinsic noise is higher than in the single RBS case and equals the Poisson value. The perfect correlation between the two protein sources (they both are translated from M) means that they are independently translated with an identical, but changing, probability per unit time, $v_1 M$. This identical probability of translation acts like the identical probability of expression in the Poisson model, and leads to the intrinsic noise being indistinguishable from the Poisson case.

Figure 2 shows the results of stochastic simulations of constitutive expression of two identical genes using the Gibson–Bruck version[13] of the Gillespie algorithm.[14] The probability of a given reaction per unit time is equal to the product of the rate constant for that reaction and the number of potential reactants present. Time steps between reactions obey a Markov process. The simple schemes of Figure 1 were initially simulated to verify both our analytical expressions and the correctness of the simulation code. It is more informative, however, to see if the expressions still hold for more detailed schemes, which contain more of the known biology and cell cycle effects. This approach was adopted for all simulations presented. For example, both the models of transcription and translation were extended to include RNAP and ribosome binding steps explicitly. Full details of the exact reactions used are given in Appendix B. The cell cycle is included through the replication of the genes of interest at some fixed time into the cycle, and by equal binomial partitioning of all protein and RNA products into the daughter cells on division. Only one daughter cell is followed, and cell volume is assumed to grow

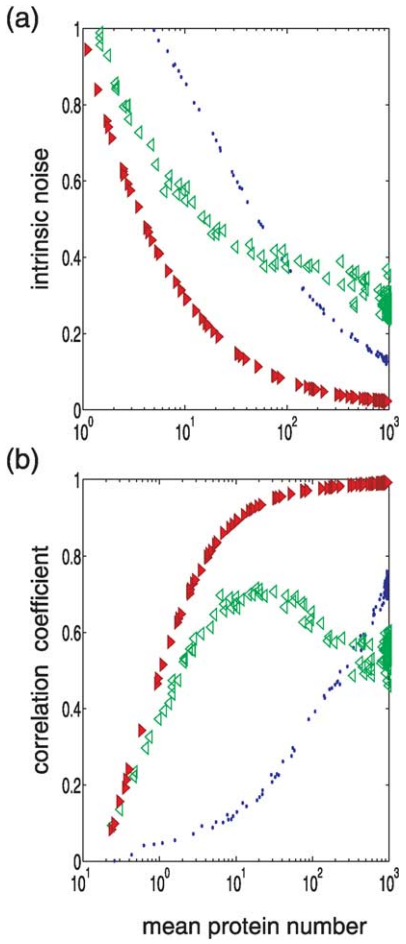

Figure 2. Noise characteristics of bicistronic encoding. (a) Intrinsic noise as a function of mean protein number. The dotted data is for two proteins encoded in two separate but identical genes (no bicistronic coding), the unfilled triangles for bicistronic coding leading to one mRNA for both proteins but with two independent RBSs, and the filled triangles indicate bicistronic coding with read-through so that only one RBS is necessary. (b) Correlation coefficient as a function of mean protein number. The symbols are the same as in (a). For both graphs, each data point is generated by simulation with a randomly chosen protein degradation rate (identical for both proteins). All other parameters are kept fixed and are given in Appendix B.

linearly[15] throughout the cycle before exactly halving at division. Following McAdams & Arkin,[16] degradosomes compete with ribosomes for the mRNA leader region. Each data point comes from a simulation with a randomly assigned protein degradation rate and all other parameters fixed (see Appendix B for numerical values).

Compared to constitutive expression of two separate, identical genes, the intrinsic noise is reduced by a factor of at least two, and sometimes three, by read-through bicistronic coding. For two RBSs, the mean levels of the two proteins are slightly different even when each protein is

expressed with identical rate constants. There is an overall bias favouring the second protein, as degradosomes (in our model) move along the mRNA preventing translation of the first gene well before the second coding region is reached, and translation prevented there. This bias causes the two protein distributions to be statistically inequivalent, and so to corresponding higher values in the intrinsic noise. With this caveat, the bicistronic encoding shown in Figure 2(a) still has lower noise levels than two gene expression for small protein numbers.

Many operons in bacteria code for enzymes involved in the same metabolic process or for components of a protein complex. In both cases, it would seem to be advantageous for the products of the operon to be positively correlated with each other. Although the intrinsic noise between two proteins is a measure of their correlation, a plot of the (Pearson) correlation coefficient is also shown in Figure 2(b). The read-through bicistronic encoding is highly correlated, and significantly more correlated than two gene expression. In general, longer living proteins (corresponding to a higher mean protein number), by averaging over many mRNA fluctuations, reduce their own stochasticity, and so generate higher correlations between themselves and other long lived proteins.

The two RBS bicistronic operon shows non-monotonic behaviour, and its parameters can be "fine-tuned" to produce optimum correlation. This finding can be understood as the consequence of two opposing phenomena: as mentioned before, a smaller protein degradation rate (and so larger mean protein numbers) reduces protein noise and acts to increase correlation. Alternatively, less protein degradation leads to greater differences between the distributions of the two proteins, A_1 and A_2. The distribution of the second encoded protein is essentially the same as the distribution of the first encoded protein, but with additional contributions arising from the extra translation of the second protein during mRNA degradation (as degradation is assumed to initiate at the first coding region). With high degradation rates, most of the A_2 proteins expressed during mRNA degradation are themselves degraded, and the distributions of the first and second encoded proteins are very similar. As the protein degradation rate drops, more and more of these "extra" proteins survive, leading to more different distributions, and to lower correlation. These two opposing behaviours (as the degradation rate is changed) lead to the correlation obtaining a maximum.

Interestingly, a two independent RBS polycistronic arrangement would not be expected to reduce stochasticity if translation dominated noise. Experimentally, then, a verification of Figure 2, using, for example, an operon encoding cyan and yellow alleles of green fluorescent protein, would strongly indicate a transcriptional origin of the noise in gene expression.

Negative Feedback and Stochasticity

Introducing auto-negative feedback, where a protein inhibits expression of its own gene, is a well-known means to reduce stochasticity. Negative transcriptional feedback is common in many bacterial operons and has been thoroughly studied.[17–20] Negative translational feedback, however, is also possible; it is thought to occur in three principle ways:[11,21] (i) *via* enhanced degradation, where binding of protein to its own mRNA prevents ribosomal access but can facilitate that of degradosomes and so reduce mRNA half-life; (ii) *via* competition, where proteins and ribosomes compete for the RBS on mRNA, with binding of protein preventing any ribosome or degradosome from binding; (iii) *via* entrapment, where protein can bind to free mRNA thus blocking the RBS, but can also bind to a ribosome occupied RBS trapping the ribosome there. For both of these binding events, we assume protein protects mRNA from degradosomes (see Figure 3(a)).

In an auto-negative transcriptional loop, repression often occurs through binding of repressor to its own promoter and either blocking the binding of RNAP or locking RNAP in an immobile state.[22] Concentrating on just the former mechanism, we use a Langevin approach (see Appendix A) to generate a mathematical description. Langevin methods assume that fluctuations do not drive the system of interest far from steady-state, and so, in our case, are strictly only valid when the numbers of molecules are not too small. However, this approach is still useful; it often works for

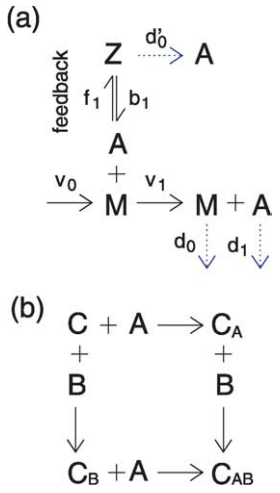

Figure 3. Reaction models. (a) Translational control. Protein A binds to the leader region of its own mRNA. For degradation-based control d'_0 is usually greater than d_0 but the case $d'_0 \leq d_0$ is also possible; for competition- and entrapment- (not shown here) based control, $d'_0 = 0$, and the mRNA/protein complex, Z, is protected from degradosomes. (b) Assembly of a macromolecular complex of three proteins. Proteins A and B bind irreversibly, and in any order, to the control protein C to form the trimer, C_{AB}.

very low numbers, and the intuition gained should nearly always be, at least, qualitatively applicable.

For transcriptional feedback, we find:

$$\eta^2_{\rm ntc} = \frac{1}{\langle A\rangle} + \frac{d_1}{d_0+d_1} \times \frac{1}{\langle M\rangle}\left\{1 - \frac{1-\epsilon_{\rm c}}{2-\epsilon_{\rm c}}\left[1+\frac{d_0}{v_1}\right]\right\} \qquad (5)$$

where $0 \le \epsilon_{\rm c} \le 1$ is inversely related to the feedback strength; $\epsilon_{\rm c} = 2/(1+\sqrt{1+4K\langle A\rangle_{\rm con}})$. Here, K is set by the repressor/DNA association constant, and the mean protein number satisfies $\langle A\rangle = \epsilon_{\rm c}\langle A\rangle_{\rm con}$, with $\langle A\rangle_{\rm con}$ its value under constitutive expression ($\langle M\rangle = \epsilon_{\rm c}\langle M\rangle_{\rm con}$ also). Comparison with (1) shows that the curly bracket term is less than one, and negative transcriptional feedback can potentially reduce noise by an amount set by the feedback strength. However, some care should be taken as mean numbers of protein and mRNA are also reduced, and are not necessarily the same as those in (1). Intuitively, negative feedback increases the probability of the promoter being repressed when protein numbers fluctuate above their mean value, and reduces this probability when protein numbers dip below the mean. It thus acts to increase the stability of the steady-state and to curtail fluctuations. Noise and transcriptional feedback have been studied, and (5) contains the results of the work done by Thattai & van Oudenaarden[10] in the limit of $K\langle A\rangle_{\rm con} \ll 1$.

Although negative transcriptional feedback can reduce noise in gene expression, most of this noise arises from mRNA fluctuations. Therefore, feedback at the level of mRNA, which reduces these fluctuations directly, should be a better noise reduction strategy. For degradation-based translational feedback, a Langevin description gives:

$$\eta^2_{\rm deg} = \frac{1}{\langle A\rangle} + \frac{d_1}{d_0+d_1}\frac{1}{\langle M\rangle} \times\left\{1 - \frac{1-\epsilon_\ell}{2-\epsilon_\ell}\left[1+\frac{d_0}{v_1}\left(1+\frac{v_1+(1-\epsilon_\ell)d_1}{d_0+\epsilon_\ell d_1}\right)\right]\right\} \qquad (6)$$

where $0 \le \epsilon_\ell \le 1$ obeys $\epsilon_\ell = 2/(1+\sqrt{1+4\mu\langle A\rangle_{\rm con}})$; see Figure 3(a) and Appendix A. In (6), μ is set by the ratio of the enhanced mRNA degradation rate when protein is bound to the mRNA to the degradation rate when protein is not bound, and by the protein/mRNA association constant; $\mu = f_1 d_0'/[(b_1+d_0')d_0]$. The mean protein (and mRNA) number is again reduced by ϵ_ℓ relative to constitutive values. An analytical result is given in Appendix A for competition-based feedback, for which noise is reduced while mRNA and protein remain at their constitutive levels. The term in round brackets in (6) must be decreased to unity to recover the transcriptional result of (5); negative translational feedback is a potentially more effective means for reducing protein noise.

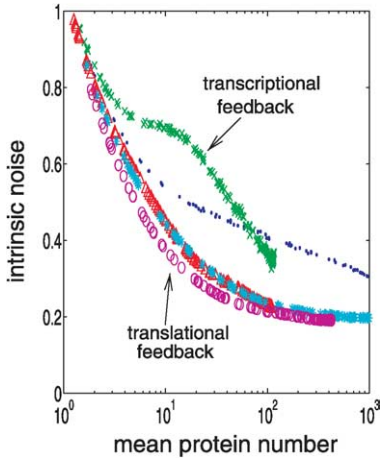

Figure 4. Intrinsic noise *versus* mean protein number for simple auto-negative genetic networks. Protein degradation rates are chosen randomly but all other parameters remain fixed for each simulation. Dots indicate constitutive expression, Xs transcriptional regulation, and triangles, stars and circles, negative degradation-based, competition-based and entrapment-based translational feedback, respectively. The three different types of translational control give very similar behaviours.

Expressions (5) and (6) both show how negative feedback reduces stochasticity by damping mRNA fluctuations (*via* the terms in curly brackets). For negative transcriptional feedback such damping is effected indirectly at the promoter and consequently is less successful than direct translational mechanisms. Figure 4 illustrates the different feedback schemes through simulation of more biologically realistic models (see Appendix B for details). The different data points are found by randomly assigning the value of the protein degradation rate, d_1 (as altering d_1 does not affect the feedback strength of the different models). Translational feedback, no matter how it is implemented, is consistently better at reducing stochasticity.

Although negative translational feedback always performs better than constitutive expression, transcriptional feedback can actually increase noise for high protein numbers. To understand this effect, (1) and (5) should be compared at different values of the parameter d_1. At equal mean protein number, $d_1^{\rm ntc}(=\epsilon_{\rm c} d_1^{\rm con})$ is less than d_1 for the corresponding constitutive case. As protein numbers are equal, only the mRNA terms matter, and $d_1^{\rm ntc} < d_1^{\rm con}$ can be shown to imply that the term outside the curly brackets is largest for the transcriptional case (noting that $\langle M\rangle$ is also reduced). However, the curly bracket term, itself, is always smaller for transcriptional feedback. For large d_1 (small protein number) the term outside the brackets dominates, and $\eta_{\rm ntc} > \eta_{\rm con}$. As d_1 decreases (and protein number increases), eventually the bracketed term gains control, and $\eta_{\rm ntc}$ falls below $\eta_{\rm con}$. The curly bracket term is considerably smaller, however, for

negative translational feedback, and η_{deg} is always less than η_{con}.

Assembly of Macromolecular Complexes

Many prokaryotic examples of translational control involve competition between regulation and function.[11] A translational repressor cannot only bind to its own mRNA (regulation), but can also interact with a substrate molecule (function). The most well-known example is, perhaps, the synthesis of ribosomal proteins, which is strongly correlated with cell growth rates.[23] Most ribosomal protein operons contain a control protein (a translational repressor), which preferentially binds to its substrate (rRNA). For low substrate concentrations, however, this repressor will bind to its own mRNA, and thus limit its own expression. Through the competition between rRNA and mRNA, ribosomal proteins are therefore only synthesized when rRNA is expressed, reducing metabolic costs and the expenditure of cellular energy. An operon that works in this way is L11, which codes for ribosomal proteins L1 and L11, and is translationally repressed by L1.[24]

Stochastic fluctuations during macromolecular complex assembly may lead to large metabolic wastage through their ability to destroy correlations between complex components.[25] Some components may be produced in excess of others, and so remain behind (presumably left for degradation) when complexes form. Although macromolecule turnover also contributes to metabolic cost, here we focus solely on stochastic fluctuations. Assembly of a heterotrimeric complex, formed from proteins *A*, *B*, and *C*, was simulated. Proteins *A* and *B* exist on a read-through operon (to ensure greater correlation between them), which is negatively controlled by *A* (control through *B*, the protein transcribed second, makes little difference). Proteins *A* and *B* irreversibly bind to protein *C*, in any order, to make the trimer, see Figure 3(b). Protein *C*, itself, is constitutively expressed. Although the trimer does not actively degrade, its numbers, like those of all proteins and RNAs, approximately halve each cell division, and the system eventually settles down to a steady-state (strictly speaking, to a limit cycle, whose period is set by the cell cycle).

To mimic metabolic changes in demand for the trimer (denoted C_{AB}), the strength of the promoter for *C* was systematically increased from low to high values. This change resulted in a corresponding increase in *C* levels. A network with a "good" design for macromolecular complex assembly was deemed one that tuned synthesis of complex components to the amount of *C* present, not through changing parameter values which were always kept fixed, but through the particular feedback mechanism it employed. To quantify such tuning, the "wastage rate" was defined as:

$$\text{wastage rate} = |\text{total amount of } A \text{ and } B \text{ synthesized per cell cycle} - \text{total amount of } C_{AB} \text{ synthesized per cell cycle}| \quad (7)$$

at steady-state. More efficient designs should produce smaller wastage rates for all possible amounts of *C*. The results are portrayed in Figure 5.

Figure 5(a) compares the mean wastage rate for the different control schemes. For low mean *C*, little *A* (the repressor) is taken up into complex, and all negatively controlled systems are almost completely repressed. Those schemes that synthesize

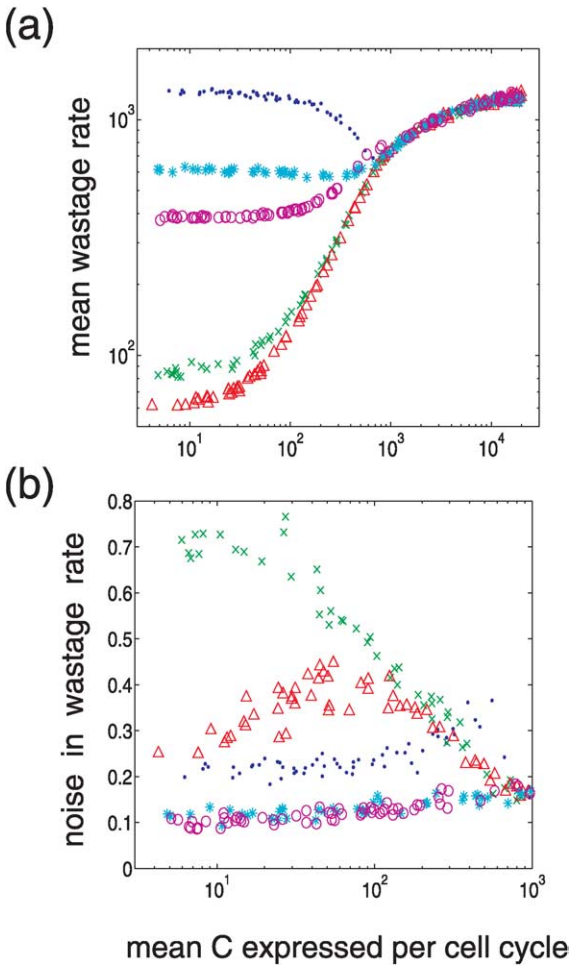

Figure 5. Efficiency of assembly of a macromolecular complex of three proteins. Proteins *A* and *B* are coded on a read-through operon, and *C* is constitutively expressed. Each data point represents one simulation run with a different promoter strength for *C* (averages are over 100 cell cycles). (a) The mean wastage rate plotted against the mean amount of *C* expressed per cell cycle. Dots denote constitutive expression of *A* and *B*, Xs indicate an *AB* operon transcriptionally repressed by protein *A*, and triangles, stars and circles an operon translationally repressed by *A* through degradation, competition and enhancement, respectively. (b) The noise in the wastage rate against the mean amount of *C* expressed per cell cycle from the same data set. Symbols are the same as in (a).

small amounts of *A* and *B* best match the low *C* levels, and have correspondingly low mean wastage rates (steady-state values, in the absence of *C*, are approximately 6000, 100, 100, 1000 and 400 for constitutive, transcriptional, and degradation-based, competition-based and entrapment-based translational feedback, respectively). Competition- and entrapment-based feedback both lead to large numbers of mRNA molecules through their protection of mRNA from degradation. Compared to transcriptionally and degradation-based translationally controlled systems, the average number of mRNAs that are being actively translated will also always be larger. These systems are therefore only able to respond to an increase in mean *C* with an excessive increase in synthesis of *A* and *B*. They are not able to fine-tune synthesis below a minimum amount set by the mean number of mRNAs. With their low protein synthesis rates, however, transcriptional and degradation-based feedback can increment synthesis at a fine enough scale to tightly match increases in mean *C*. Consequently, they have low wastage rates. Finally, at high mean *C*, all *A* is involved in complex formation, and each system is completely de-repressed with its curve collapsing onto the constitutive data.

The large numbers of mRNAs for the competition- and entrapment-based schemes do, however, reduce the noise in the wastage rate; see Figure 5(b). Interestingly, the degradation-based scheme has the lowest mean wastage rate and has significantly less noise than transcriptional feedback (the other scheme with low wastage). In this sense, degradation-based negative translational feedback best coordinates operon expression with a control protein. Unlike transcriptional feedback, degradation-based feedback also has an additional parameter besides the repressor/nucleic acid binding strength. If the mRNA degradation rate induced by protein binding in this scheme is increased by a factor of ten, the mean wastage ratio becomes up to half that of transcription and the noise in the wastage rate, although rising, still remains below transcriptional levels (data not shown).

Discussion

Intrinsic noise is usually set by transcription, which generates significant fluctuations in mRNA molecules.[8,9] Here, we argue that direct reduction of these fluctuations, through translational control, is most effective at attenuating noise. This effect has been, perhaps, most exploited by the extensive coding of prokaryotic genes in operons. Although there are many other advantages to operon structure,[26] it can also reduce intrinsic noise between operon proteins (see Figure 2). This increased protein correlation should boost cellular efficiency if the operon codes for a series of enzymes targeted at synthesizing one substrate, such as the tryptophan operon, or for a components of a larger structure, e.g. the flagellar operons.

Auto-negative feedback loops involving translational feedback are significantly more efficient at reducing fluctuations than transcriptional repression (Figure 4). Translational control has received less attention in the literature but a number of examples stand out. The protein, Hfq (also called HF-I), is an RNA-binding protein whose disruption causes pronounced cellular effects, such as decreased growth rate, osmosensitivity, and increased cell length.[27] It has been suggested to play a global regulatory role, possibly through its positive regulation of *rpoS* sigma factor,[28] and is known to undergo degradation-based translational auto-repression.[29] For such a global regulator, large fluctuations appear to be deleterious to the cell and translational repression may have been selected to tightly limit Hfq levels. Similarly, the two RNases, RNase E and RNase III, which are responsible for most RNA degradation, both negatively translationally autoregulate themselves through degradation (as opposed to regulating each other, or transcriptional regulation).[30,31] Such regulation strongly reduces noise, which is potentially damaging as over expression of RNase E severely affects *E. coli*.[32]

Degradation-based negative translational feedback also provides better coupling between operon expression and a control protein during macromolecular complex assembly (Figure 5). It produces a low mean rate of metabolic expenditure (wastage) with small fluctuations around this mean. A possible example is ribosome assembly, where translational feedback is common. The L11 ribosomal protein operon, whose L1 protein is known to bind competitively to rRNA and its own mRNA, also carries out its translational repression through a form of enhanced degradation.[33]

Translational feedback as a genetic design has a strong ability to regulate stochastic fluctuations. Proteins that play a global regulatory role might be expected to deleteriously affect cellular behaviour if their numbers fluctuate in an uncontrolled manner. If we accept that negative feedback has been selected to reduce unwanted stochasticity, then translational feedback may have been adopted more frequently for those proteins that act globally. Transcriptional feedback, with its low mRNA turnover and so reduced metabolic cost, may be more suited for those operons with insulated cellular tasks.

Acknowledgements

P.S.S. thanks Leon Glass, Eric Libby, Mike Mackey, Ted Perkins, Sharad Ramanathan, and particularly Eric Siggia for useful comments. This work was supported by a Tier II Canada Research Chair and by NSERC.

Appendix A: Langevin theory

Here, we present a derivation of the analytical expressions given in the text. Equations (1), (3) and (4) are derived by direct solution for the moments of the master equation using the standard generating function method.[8,12] Introducing feedback adds non-linearity, and the master equation often becomes intractable. The Langevin approximation, however, does provide a solution, at least for small fluctuations around steady-state. Our approach is based on that of Renshaw,[34] which we find more intuitive than the usual Langevin description (i.e. Fokker–Planck type solutions of the master equation). Our method is equivalent to these techniques and to the linear noise approximation,[12] at least, at steady-state.

In Figure 3(a), for example, there are three variables (protein, A, mRNA, M, and mRNA/protein complex, Z), which in a Langevin description lead to three differential equations, each with its associated noise term:

$$\begin{aligned}\frac{\mathrm{d}Z}{\mathrm{d}t} &= f_1AM - b_1Z - d_0'Z + \xi_1,\\ \frac{\mathrm{d}M}{\mathrm{d}t} &= v_0 - d_0M + b_1Z - f_1AM + \xi_2,\\ \frac{\mathrm{d}A}{\mathrm{d}t} &= v_1M - d_1A + b_1Z + d_0'Z - f_1AM + \xi_3 \end{aligned} \quad \text{(A1)}$$

where Z, M, and A are also used to denote the number of molecules of Z, M, and A, respectively. The ξ_i are random variables, and allow the modelling of thermal fluctuations and stochasticity when appropriately defined. For intrinsic noise, the noise terms are additive in (A1). Multiplicative noise, however, can also be expected when extrinsic variables are included.

To choose the ξ_i distributions, let Z^s, M^s, and A^s denote the amounts of Z, M, and A at steady-state (when all time derivatives are zero). Then, for a time interval δt so small that only one reaction can occur, $\xi_i\delta t$, for $i=1,2,3$, can only be ±1 or zero. Let $P(j,k,\ell)$ be the probability that $\xi_1\delta t=j$, $\xi_2\delta t=k$, and $\xi_3\delta t=\ell$. From Figure 3(a), one has:

$$\begin{aligned} P(1,-1,-1) &= f_1A^sM^s\delta t\\ P(-1,1,1) &= b_1Z^s\delta t\\ P(-1,0,1) &= d_0'Z^s\delta t\\ P(0,1,0) &= v_0\delta t\\ P(0,-1,0) &= d_0M^s\delta t\\ P(0,0,1) &= v_1M^s\delta t\\ P(0,0,-1) &= d_1A^s\delta t \end{aligned} \quad \text{(A2)}$$

at steady-state, with all other $P(j,k,\ell)$ identically equal to zero. Equation (A2) implies that the mean value of ξ_2, for example, obeys:

$$\begin{aligned}\langle\xi_2(t)\delta t\rangle &= (-1)f_1A^sM^s\delta t + (+1)b_1Z^s\delta t\\ &\quad + (+1)v_0\delta t + (-1)d_0M^s\delta t = 0\end{aligned} \quad \text{(A3)}$$

from (A1) (evaluated at steady-state). Similarly, the mean square satisfies:

$$\begin{aligned}\langle\xi_2^2(t)\delta t^2\rangle &= (-1)^2f_1A^sM^s\delta t + (+1)^2b_1Z^s\delta t\\ &\quad + (+1)^2v_0\delta t + (-1)^2d_0M^s\delta t\end{aligned} \quad \text{(A4)}$$

and so:

$$\langle\xi_2^2(t)\rangle\delta t = 2(d_0 + f_1A^s)M^s \quad \text{(A5)}$$

again using (A1). If we assume that the steady-state values are large enough, then typical fluctuations away from these values will always be small compared to the values themselves. In that case, (A2) will be approximately obeyed for all time intervals of size δt, and consequently $\xi_i(t_1)$ will be uncorrelated with $\xi_i(t_2)$ for all $|t_1-t_2|>\delta t$. This lack of correlation for $t_1\neq t_2$ can be mathematically described by a delta function. Thus, in total, the ξ_i can be shown to satisfy:

$$\langle\xi_1\rangle = \langle\xi_2\rangle = \langle\xi_3\rangle = 0 \quad \text{(A6)}$$

with:

$$\begin{aligned}\langle\xi_1(t_1)\xi_1(t_2)\rangle &= 2(b_1 + d_0')Z^s\delta(t_1-t_2),\\ \langle\xi_2(t_1)\xi_2(t_2)\rangle &= 2(d_0 + f_1A^s)M^s\delta(t_1-t_2),\\ \langle\xi_3(t_1)\xi_3(t_2)\rangle &= 2(d_1 + f_1M^s)A^s\delta(t_1-t_2)\end{aligned} \quad \text{(A7)}$$

and the cross-correlations:

$$\begin{aligned}\langle\xi_1(t_1)\xi_2(t_2)\rangle &= -(2b_1 + d_0')Z^s\delta(t_1-t_2),\\ \langle\xi_1(t_1)\xi_3(t_2)\rangle &= -2(b_1 + d_0')Z^s\delta(t_1-t_2),\\ \langle\xi_2(t_1)\xi_3(t_2)\rangle &= (2b_1 + d_0')Z^s\delta(t_1-t_2)\end{aligned} \quad \text{(A8)}$$

Equations (A1), (A6)–(A8) together specify our model of translational feedback. Linearizing (A1) around the steady-state values of Z^s, M^s and A^s allows complete solution of the problem in principle.

In general, linearization of the equations of motion around steady-state leads to:

$$\frac{\mathrm{d}}{\mathrm{d}t}\mathbf{X} = A(\mathbf{X}-\mathbf{X}^s) + \xi(t) \quad \text{(A9)}$$

for some chemical species X_i, and where A is a matrix of first-order derivatives evaluated at steady-state. The means of the ξ_i are defined to be zero, and their cross-correlations obey:

$$\langle\xi_i(t_1)\xi_j(t_2)\rangle = \Gamma_{ij}\delta(t_1-t_2) \quad \text{(A10)}$$

for some constant matrix Γ. If B_{ij} is an eigenvector of A with eigenvalue $\lambda^{(k)}$ such that:

$$\sum_j A_{ij}B_{jk} = \lambda^{(k)}B_{ik} \quad \text{(A11)}$$

then standard linear algebra gives:

$$\langle X_i(t)\rangle = X_i^{\mathrm{s}} - \sum_{j,k} B_{ij} \mathrm{e}^{\lambda^{(j)} t} B_{jk}^{-1} X_k^{\mathrm{s}} \tag{A12}$$

for the initial condition $\langle X_i(0)\rangle = 0$. Correlations between the X_i satisfy:

$$\langle [X_i(t_1) - \langle X_i(t_1)\rangle][X_j(t_2) - \langle X_j(t_2)\rangle]\rangle$$

$$= \sum_{p,q,r,s} B_{ip} B_{jr} \frac{\Gamma_{qs}}{\lambda^{(p)} + \lambda^{(r)}} \left[\mathrm{e}^{\lambda^{(p)} t_1 + \lambda^{(r)} t_2} - \mathrm{e}^{\lambda^{(p)}(t_1 - t_2)}\right]$$

$$\times B_{pq}^{-1} B_{rs}^{-1} \tag{A13}$$

for $t_1 \geq t_2$, and so at steady-state:

$$\langle [X_i - \langle X_i\rangle][X_j - \langle X_j\rangle]\rangle$$

$$= -\sum_{p,q,r,s} B_{ip} B_{jr} \frac{\Gamma_{qs}}{\lambda^{(p)} + \lambda^{(r)}} B_{pq}^{-1} B_{rs}^{-1} \tag{A14}$$

Equation (A14) allows stochastic effects to be determined for any Langevin system. However, it requires calculation of the time-scales $\lambda^{(i)}$, which set auto-correlation times, for example. Such a calculation can involve the analytical solution of high order polynomials, and so is often not very illuminating, even if possible.

In Figure 3(a), if $d'_0 > d_0$ the life-time of Z will be shorter than those of M and A. This difference in time-scales permits $\mathrm{d}Z/\mathrm{d}t$ to be approximately set to zero, and to Z obeying:

$$Z = \frac{f_1 AM + \xi_1}{b_1 + d'_0} \tag{A15}$$

from (A1). Then, M and A obey:

$$\frac{\mathrm{d}M}{\mathrm{d}t} = v_0 - d_0 M - \frac{d'_0 f_1 AM}{b_1 + d'_0} + \chi_1,$$

$$\frac{\mathrm{d}A}{\mathrm{d}t} = v_1 M - d_1 A + \chi_2 \tag{A16}$$

where:

$$\chi_1 = \frac{b_1 \xi_1}{b_1 + d'_0} + \xi_2, \quad \chi_2 = \xi_1 + \xi_3 \tag{A17}$$

The properties of these two new random variables can be determined from (A7) and (A8):

$$\langle \chi_1(t_1)\chi_1(t_2)\rangle = 2(d_0 + d_1 A^{\mathrm{s}}) M^{\mathrm{s}} \delta(t_1 - t_2),$$

$$\langle \chi_2(t_1)\chi_2(t_2)\rangle = 2 d_1 A^{\mathrm{s}} \delta(t_1 - t_2),$$

$$\langle \chi_1(t_1)\chi_2(t_2)\rangle = 0 \tag{A18}$$

The time-scale difference allows (A1) to be reduced to two equations; equation (A14) therefore becomes straightforward to evaluate (only a quadratic equation for the eigenvalues must be solved). Matrix A is found by linearizing (A16) around steady-state, and the Γ_{ij} are given by (A18) leading to (6).

For competition-based translational feedback

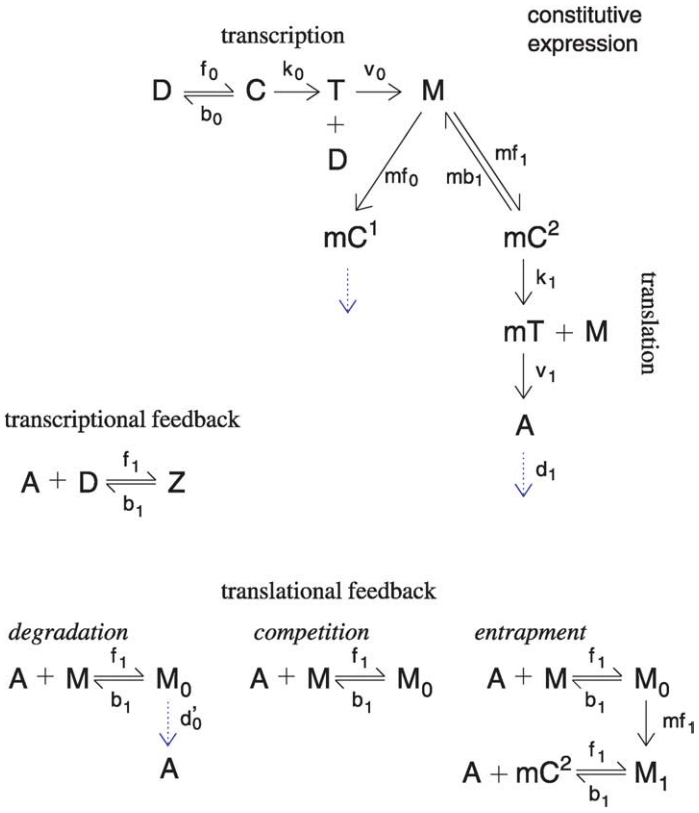

Figure B1. Reaction scheme for gene expression with various types of autogenous control. Transcription is modelled[35] as reversible binding of RNAP to promoter, D, (rates f_0 and b_0). Isomerization from closed to open complex and initiation of transcription are all approximated as a first-order process (rate k_0). The simulation keeps track of only the leader region of the mRNA, M, which is made by transcribing polymerase, T, at rate v_0. mRNA is degraded following the binding of degradosomes (rate mf_0) to form complex mC^1, which eventually decays. Following McAdams & Arkin[16] ribosomes compete with degradosomes for leader mRNA and bind reversibly (rates mf_1 and mb_1). Start of translation is from the mC^2 state with rate k_1, which then frees M for further binding. Protein is translated (rate v_1) in the mT state, and decays with rate d_1 once synthesized. For transcriptional feedback, protein binds to the promoter and sequesters it in complex Z. Translational feedback can proceed in three ways: degradation-based, with protein/RNA complex, M_0, decaying to protein, competition-based, and entrapment-based, where protein binds reversibly to both leader mRNA, M, and to leader mRNA/ribosome complex, mC^2.

$d'_0 = 0$, and mRNA is the most short-lived species. By setting dM/dt to zero, the intrinsic noise can be found to be:

$$\eta^2_{\rm com} = \frac{1}{\langle A\rangle} + \frac{d_1}{d_0 + d_1} \times \frac{1}{\langle M\rangle}\left[1 - \frac{2H(1 + v_1/d_0)}{1 + H(1 + 2v_1/d_0)}\right] \qquad \text{(A19)}$$

with the protein/mRNA association constant $H = f_1 M^s/b_1$. Both mean protein and mean mRNA, however, retain their constitutive values. Equation (A19), due to the presence of the negative term, is less noisy than constitutive expression.

Equation (5) is derived similarly.

Appendix B: Computer simulations

All simulations are based around the model for constitutive expression shown in Figure B1. Reactions were simulated using the Gibson–Bruck version[13] of the Gillespie algorithm.[14] Each gene,

Table B1. Parameters suitable for gene expression in *E. coli*

Process	Parameters
RNAP binding to DNA	Free RNAP concentration = 30 nM,[36] binding rate 1.4×10^7 M^{-1} s^{-1} for λP_L[37] $\Rightarrow f_0 = 0.42$ s^{-1}, $b_0 = 0.1$ s^{-1} (to give an equilibrium constant of 1.4×10^8 M^{-1} [36])
Transcription initiation rate	$k_0 = 0.1$ s^{-1} [38] (closed to open complex isomerization)
Formation and degradation of RBS on mRNA	$v_0 = 0.3$ s^{-1} (RNAP moving at 40 nt s^{-1} [39]), $mf_0 = 0.114$ s^{-1} (so average number of proteins per constitutive transcript is 15)
Binding of ribosome	Free ribosome concentration = 400 nM (order of magnitude larger than RNAP) binding rate 1×10^7 M^{-1} s^{-1} $\Rightarrow mf_1 = 4.0$ s^{-1}, $mb_1 = 0.4$ s^{-1} (to give an equilibrium constant of 2.5×10^7 M^{-1} [40])
Translation	$k_1 = 0.3$ s^{-1}, [40] $v_1 = 0.04$ s^{-1} (for a 1000 nt protein and a translation rate of 40 nt s^{-1} [23])
Protein degradation	$d_1 = 6.42\times10^{-5}$ s^{-1} ($t_{1/2} \simeq 3$ hours
Cell cycle time	$T = 60$ minutes (for at most two chromosomes per cell)
Gene replication time	$t_d = 0.4T$ (arbitrarily chosen)
Nucleic acid binding	$f_1 = 10^9$ M^{-1} s^{-1} (diffusion limited), $b_1 = 0.215$ s^{-1}
Induced degradation	$d'_0 = 0.444$ s^{-1} (different feedbacks are of equal strength)

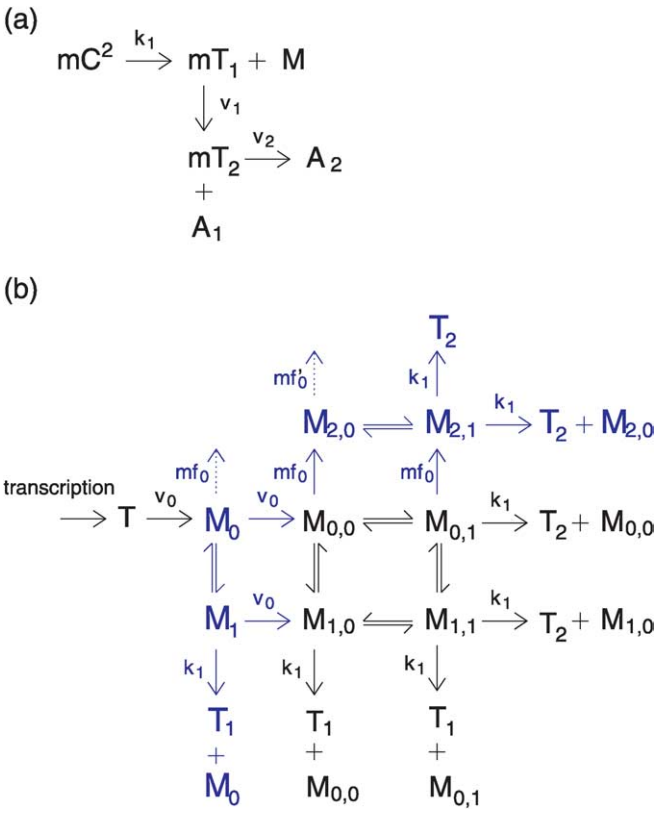

Figure B2. Reactions schemes for bicistronic operons. Both schemes are based on that of constitutive expression shown in Figure B1, and have identical models for transcription. (a) A "read-through" operon for which only the first cistron has a RBS. A translating ribosome, mT_1, releases protein A_1 before translating protein A_2 (in the state mT_2). (b) An operon with two independent RBSs. A fully transcribed mRNA is denoted with the symbol M with two subscripts. The first and second subscripts denote the occupancy of the first and second RBSs, respectively; 0 indicating a free site; 1, a bound ribosome; and 2, a bound degradosome. The rates of ribosome association and deassociation, which are not explicitly labelled in the Figure, are mf_1 and mb_1. Translating ribosomes are denoted as T_1 and T_2, and translate mRNA to proteins A_1 and A_2, respectively. Translation takes place with rate v_1 as in Figure B1. Due to the direction of motion of the degradosome, some translation of A_2 can still take place during mRNA decay as shown in the upper part of the diagram. Transcription of DNA takes place in two steps, with M_i and $M_{i,j}$ being mRNA for which one RBS or two RBSs have been transcribed, respectively. Competition for M_0 between ribosomes, leading to the state M_1, and degradosomes occurs immediately. For clarity, all the rate constants for A_2 have been set to be identical with those of A_1. Parameters are given in Table B1 except $mf'_0 = 0.04$ s^{-1}.

state D in Figure B1, is replicated at a fixed time, t_d, into each cell cycle. Both RNA and protein are partitioned with equal probability into the daughter cells on division, while the number of DNA states is exactly halved. Parameter values, typical for *E. coli* are given in Table B1. Rates related to feedback are chosen to ensure that:

$$K = \frac{(b_0 + k_0)f_1}{(b_0 + k_0 + f_0)b_1} = \frac{d_0' f_1}{(b_1 + d_0')d_0} = \mu \qquad \text{(B1)}$$

i.e. that the feedback strengths for transcriptional and degradation-based translational control are equal.

For bicistronic encoding, the translation scheme used in the model of constitutive expression was modified (Figure B2). In the two RBS model, timing variables were also included to ensure that mRNA synthesis and degradation occurred correctly. For example, one such variable acted to maintain a well-defined time for synthesis of the second RBS during transcription.

References

1. Guptasarma, P. (1995). Does replication-induced transcription regulate synthesis of the myriad low copy number proteins of *Escherichia coli*. *Bioessays*, **17**, 987–997.
2. Elowitz, M. B., Levine, A. J., Siggia, E. D. & Swain, P. S. (2002). Stochastic gene expression in a single cell. *Science*, **297**, 1183–1186.
3. Barkai, N. & Leibler, S. (2000). Circadian clocks limited by noise. *Nature*, **403**, 267–268.
4. Vilar, J. M., Kueh, H. Y., Barkai, N. & Leibler, S. (2002). Mechanisms of noise-resistance in genetic oscillators. *Proc. Natl Acad. Sci. USA*, **99**, 5988–5992.
5. Bundschuh, R., Hayot, F. & Jayaprakash, C. (2003). The role of dimerization in noise reduction of simple genetic networks. *J. Theoret. Biol.* **220**, 261–269.
6. Vilar, J. M. & Leibler, S. (2003). DNA looping and physical constraints on transcription regulation. *J. Mol. Biol.* **331**, 981–989.
7. Thattai, M. & van Oudenaarden, A. (2002). Attenuation of noise in ultrasensitive signaling cascades. *Biophys. J.* **82**, 2943–2950.
8. Swain, P. S., Elowitz, M. B. & Siggia, E. D. (2002). Intrinsic and extrinsic contributions to stochasticity in gene expression. *Proc. Natl Acad. Sci. USA*, **99**, 12795–12800.
9. Paulsson, J. (2004). Summing up the noise in gene networks. *Nature*, **427**, 415–418.
10. Thattai, M. & van Oudenaarden, A. (2001). Intrinsic noise in gene regulatory networks. *Proc. Natl Acad. Sci. USA*, **98**, 8614–8619.
11. Springer, M. (1996). Translational control of gene expression in *E. coli* and bacteriophage. In *Regulation of Gene Expression in* Escherichia coli (Lin, E. C. C. & Simon-Lynch, A., eds), pp. 85–126, Kluwer, New York.
12. van Kampen, N. G. (1990). *Stochastic Processes in Physics and Chemistry*. Elsevier, New York.
13. Gibson, M. A. & Bruck, J. (2000). Efficient exact stochastic simulation of chemical systems with many species and many channels. *J. Phys. Chem. A*, **104**, 1876–1889.
14. Gillespie, D. (1977). Exact stochastic simulation of coupled chemical-reactions. *J. Phys. Chem.* **81**, 2340–2361.
15. Kubitschek, H. E. (1990). Cell volume increase in *Escherichia coli* after shifts to richer media. *J. Bacteriol.* **172**, 94–101.
16. McAdams, H. H. & Arkin, A. (1997). Stochastic mechanisms in gene expression. *Proc. Natl Acad. Sci. USA*, **94**, 814–819.
17. Savageau, M. A. (1974). Comparison of classical and autogenous systems of regulation in inducible operons. *Nature*, **252**, 546–549.
18. Becskei, A. & Serrano, L. (2000). Engineering stability in gene networks by autoregulation. *Nature*, **405**, 590–593.
19. Rosenfeld, N., Elowitz, M. B. & Alon, U. (2002). Negative autoregulation speeds the response times of transcription networks. *J. Mol. Biol.* **323**, 785–793.
20. Isaacs, F. J., Hasty, J., Cantor, C. R. & Collins, J. J. (2003). Prediction and measurement of an autoregulatory genetic module. *Proc. Natl Acad. Sci. USA*, **100**, 7714–7719.
21. Draper, D. E. (1987). Translational regulation of ribosomal proteins in *E. coli*. In *Translational Regulation of Gene Expression* (Ilan, J., ed.), pp. 1–25, Plenum Press, New York.
22. Ptashne, M. (1992). *A Genetic Switch*. Cell Press/ Blackwell Scientific Publications, Cambridge, MA.
23. Bremer, H. & Dennis, P. P. (1996). Modulation of chemical composition and other parameters of the cell by growth rate. In Escherichia coli *and* Salmonella: *Cellular and Molecular Biology* (Neidhardt, F. C., ed.), pp. 1553–1569, ASM Press, Washington, DC.
24. Cole, J. R. & Nomura, M. (1986). Translational regulation is responsible for growth-rate-dependent and stringent control of the synthesis of ribosomal proteins L11 and L1 in *Escherichia coli*. *Proc. Natl Acad. Sci. USA*, **83**, 4129–4133.
25. Fraser, H. B., Hirsh, A. E., Giaever, G., Kumm, J. & Eisen, M. B. (2004). Noise minimization in eukaryotic gene expression, PLoS. *Biology*, **2**, 834–838.
26. McAdams, H. H., Srinivasan, B. & Arkin, A. P. (2004). The evolution of genetic regulatory systems in bacteria. *Nature Rev. Genet.* **5**, 169–178.
27. Tsui, H. C., Leung, H. C. & Winkler, M. E. (1994). Characterization of broadly pleiotropic phenotypes caused by an hfq insertion mutation in *Escherichia coli* K-12. *Mol. Microbiol.* **13**, 35–49.
28. Muffler, A., Traulsen, D. D., Fischer, D., Lange, R. & Hengge-Aronis, R. (1997). The RNA-binding protein HF-I plays a global regulatory role which is largely, but not exclusively, due to its role in expression of the sigmaS subunit of RNA polymerase in *Escherichia coli*. *J. Bacteriol.* **179**, 297–300.
29. Tsui, H. C., Feng, G. & Winkler, M. E. (1997). Negative regulation of mutS and mutH repair gene expression by the Hfq and RpoS global regulators of *Escherichia coli* K-12. *J. Bacteriol.* **179**, 7476–7487.
30. Jain, C. & Belasco, J. G. (1995). RNase E autoregulates its synthesis by controlling the degradation rate of its own mRNA in *Escherichia coli*: unusual sensitivity of the rne transcript to RNase. *Genes Dev.* **9**, 84–96.
31. Bardwell, J. C., Regnier, P., Chen, S. M., Nakamura, Y., Grunberg-Manago, M. & Court, D. L. (1989). Autoregulation of RNase III operon by mRNA processing. *EMBO J.* **8**, 3401–3407.
32. Claverie-Martin, F., Diaz-Torres, M. R., Yancey, S. D. &

Kushner, S. R. (1991). Analysis of the altered mRNA stability (ams) gene from *Escherichia coli*. *J. Biol. Chem.* **266**, 2843–2851.
33. Cole, J. R. & Nomura, M. (1986). Changes in the half-life of ribosomal protein messenger RNA caused by translational repression. *J. Mol. Biol.* **188**, 383–392.
34. Renshaw, E. (1991). *Modelling Biological Populations in Space and Time*. Cambridge University Press, New York.
35. Record, T. M., Reznikoff, W. A., Craig, M. L., McQuade, K. L. & Schlax, P. J. (1996). *Escherichia coli* RNA polymerase (Eσ70), promotors, and the kinetics of the steps of transcription initiation. In Escherichia coli *and* Salmonella: *Cellular and Molecular Biology* (Neidhardt, F. C., ed.), pp. 792–821, ASM press, Washington, DC.
36. McClure, W. R. (1983). A biochemical analysis of the effect of RNA polymerase concentration on the *in vivo* control of RNA chain initiation frequency. In *Biochemistry of Metabolic Processes* (Lennon, D. L. F., Stratman, F. W. & Zahlten, R. N., eds), pp. 207–217, Elsevier, New York.
37. Lanzer, M. & Bujard, H. (1988). Promoters largely determine the efficiency of repressor action. *Proc. Natl Acad. Sci. USA*, **85**, 8973–8977.
38. Hawley, D. K. & McClure, W. R. (1982). Mechanism of activation of transcription initiation from the lambda P_{RM} promoter. *J. Mol. Biol.* **157**, 493–525.
39. Manor, H., Goodman, D. & Stent, G. S. (1969). RNA chain growth rates in *Escherichia coli*. *J. Mol. Biol.* **39**, 1–29.
40. Draper, D. E. (1996). Translation initiation. In Escherichia coli *and* Salmonella: *Cellular and Molecular Biology* (Neidhardt, F. C., ed.), pp. 902–908, ASM press, Washington, DC.

Edited by D. E. Draper

(Received 2 August 2004; received in revised form 21 September 2004; accepted 24 September 2004)